

Structure and stability of the interface between a strained crystal and a shearing liquid

Scott Butler and Peter Harrowell*

School of Chemistry, University of Sydney, New South Wales 2006, Australia

(Received 13 November 2002; published 22 May 2003)

The results are presented from nonequilibrium molecular dynamics simulations of the stationary nonequilibrium interface between a shearing liquid and its strained crystal. The penetration of the velocity field into the crystal is shown to increase with an increasing shear stress along the coexistence line. Slip and creep compensate within the interfacial region to produce an effective flow boundary well described, macroscopically, by a standard stick boundary condition. The shear flow within the interface is found to involve intermittent stick-slip motion, with the slip accompanied by disordering. A theoretical treatment of the interfacial stability is proposed, based on the competing rates of crystallization and erosion, and is found to provide a reasonable representation of the simulated stress-temperature phase diagram.

DOI: 10.1103/PhysRevE.67.051503

PACS number(s): 83.10.Rs, 64.60.-i, 05.20.-y, 83.60.Rs

I. INTRODUCTION

In this paper, we consider the behavior of the crystal-melt interface when subjected to a shear stress. Unlike the sharp solid-liquid interface between two substances with widely differing melting points, the crystal-melt interface is structurally diffuse, extending over 3–10 molecular diameters. What kind of boundary does such a fragile interface pose for the flow field? What influence does this flow have back on the interface itself? There is considerable interest in using computer simulations to understand the molecular nature of the liquid velocity and stress fields in the vicinity of solid walls [1]. The problem we consider here is rather different due to the proximity to the solid's melting point. It is possible, for example, to completely melt the solid if a sufficiently high shear rate is imposed on the liquid.

In Refs. [2,3], we have reported the stable coexistence between a strained crystal made up of Lennard-Jones particles and its shearing melt as observed in nonequilibrium molecular dynamics (NEMD) simulations. We have demonstrated that the nonequilibrium coexistence can neither arise from the mechanical instability of the bulk solid nor from the minimization of some nonequilibrium analog of a free energy. The reader is referred to these papers for details of this argument. At equilibrium, coexistence is determined by the condition that the chemical potentials of the two phases be equal. In the case of the nonequilibrium coexistence between crystal and liquid, we have eliminated any extension of this condition to include nonequilibrium analogs of the chemical potential of the bulk phases. Instead, we must replace the condition of chemical potential equality with the more general condition that the nonequilibrium crystal-liquid interface is stationary. Previously, Olmsted and Lu [4] have argued that phase coexistence in a liquid of rigid rods under shear requires the inclusion of gradient terms in the equations of motion. The apparent generality of the importance of the interfacial regions in establishing coexistence under shear motivates this NEMD study of a stationary nonequilibrium

interface. In this paper, we explore the structure and fluctuations of the crystal-liquid interface along the nonequilibrium coexistence line. We propose that the observed nonequilibrium coexistence is the result of balancing the rate of crystal growth with the rate of surface erosion by the shearing liquid [2].

II. ALGORITHM AND METHODOLOGY

The model and algorithm have been described in some detail previously [2,3], and so we present here only a summary of our calculations. Our simulations involve the integration of classical equations of motion for $N=2592$ particles interacting via a 12-6 Lennard-Jones potential $\phi(r)$,

$$\phi(r) = 4\epsilon[(a/r)^{12} - (a/r)^6]. \quad (1)$$

The following units are used throughout the paper: time t is in units of $\tau = a(m/\epsilon)^{1/2}$, mass has units of m , distance r is in units of a , the temperature T is in units of ϵ/k_B , and pressure and stress are in units of ϵ/a^2 . For reference, the average collision time (defined as the first zero of the velocity autocorrelation function) is $\sim 0.1\tau$.

Periodic boundary conditions apply along the x and z axes. Walls bound either end of the cell along the y axis. The walls were modeled by pinning particles to specified positions, either those of a perfect (111) layer of the face-centered-cubic (fcc) lattice or to those of a single liquid configuration, via a harmonic potential. The spring constant used for this potential was $k_{spring} = 57.1$. Wall particles also interact with each other and the liquid particles by the same Lennard-Jones potential as govern the liquid-liquid interactions.

All of the results presented are for a normal pressure $P_{yy} = 3.5$ and a time step of $\Delta t = 0.004$. A constant shear rate was applied by moving each wall by a displacement of $\Delta x = 0.5\dot{\gamma}L_y\Delta t$ per time step in opposite directions, where $\dot{\gamma}$ is the applied shear rate, L_y is the distance between the walls, and Δt is the time step. The crystalline wall was aligned such that the shear gradient lies normal to the (111) plane, while the shear flow direction (along the x axis) lies parallel to the easy slip (011) direction.

*Author to whom correspondence should be addressed. Electronic address: peter@chem.usyd.edu.au

Two types of thermostats have been used, a wall thermostat and a homogeneous thermostat. The wall thermostat rescaled only the temperature of the wall particles, system particles being indirectly thermostated through collision with the walls. The temperature was calculated using

$$T_{wall} = \frac{1}{3N_{wall}} \left(\sum_{i=1}^{N_{wall}} p_{ix}^2 + p_{iy}^2 + p_{iz}^2 \right), \quad (2)$$

where p_{ix} refers to the x component of the momentum of particle i and N_{wall} is the number of particles in the wall. This method of thermostating produces a temperature gradient between the heat source, in this case the frictional heating in a shearing liquid, and the heat sinks in the walls. An alternative thermostat avoids this gradient by applying a homogeneous rescaling of the components of the particle momenta along the shear gradient (y) and vorticity (z) directions. To accommodate the spatial variation in the two-phase system, we divided the cell into layers in the x - z plane, the height of each layer is equal to the spacing between fcc (111) layers in the perfect crystal structure. For each cell, the average momenta $\langle p_y \rangle_{cell}$ and $\langle p_z \rangle_{cell}$ was calculated, and the values of p_y and p_z for each particle within the layer were rescaled to maintain a constant temperature in these components. As reported in Refs. [2,3], we find no effect of the thermostat choice on the position of the nonequilibrium solid-liquid coexistence line *if* the interfacial temperature is used as the system temperature in the case of wall thermostats.

The instantaneous normal pressure P_{yy} was calculated using the expression

$$P_{yy} = \frac{1}{V} \sum_i q_{iy} F_{iy} + \sum_i p_{iy}^2, \quad (3)$$

where F_{iy} and q_{iy} are the component of the total force on particle i and the position vectors for particle i along the y Cartesian axes, respectively. A Nosé-Hoover algorithm [5] was used to hold the average value of P_{yy} constant, the time evolution of the y dimension of the cell, L_y , being

$$\frac{dL_y}{dt} = \frac{1}{Q_p} (P_{yy} - P_{yy}^0), \quad (4)$$

where L_y is the y dimension of the cell, P_{yy} is the instantaneous value of the normal pressure, P_{yy}^0 is the desired normal pressure, and Q_p determines the rate at which excursions from the target value are damped. A value of $Q_p = 10$ was used in all constant P_{yy} simulations.

III. STRUCTURE AND FLOW AT THE STATIONARY NONEQUILIBRIUM INTERFACE

A. The nonequilibrium coexistence curve

In Refs. [2,3] we established that the Lennard-Jones liquid under shear can coexist with its crystalline solid. Specifically, we studied the fcc crystal whose interface was parallel to the (111) plane and with shear flow parallel to the (110) direction. The plot of the coexistence shear stress against tempera-

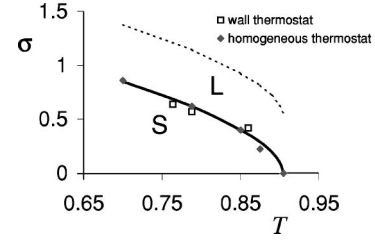


FIG. 1. The shear stress σ at crystal-liquid coexistence as a function of temperature T . (The solid line is simply a guide to the eye.) Data obtained from wall and homogeneous thermostats are included. In the former case, where there is a temperature gradient, we have used the interfacial temperature to define the appropriate temperature for the state. The crystal yield stress is shown as a dashed line.

ture, presented in Fig. 1, can be interpreted as a nonequilibrium phase diagram in the stress-temperature plane [3]. (The dashed line in Fig. 1 corresponds to the yield stress of the bulk crystal [3].) We have shown [2,3] that the relative volumes of the two phases obeys a standard lever rule with respect to the overall shear rate of the sample. We shall now examine the crystal-liquid interface at a number of points along the nonequilibrium coexistence line.

B. Interface structure

To measure the in-plane hexagonal order within layers parallel to the walls, we introduce $X(l)$, the in-plane order of the l th layer, defined as

$$X(l) = \frac{1}{N_l} \sum_{i=1}^{N_l} \frac{1}{N_i(N_i-1)} \sum_{j=1}^{N_i} \sum_{k \neq j}^{N_i} \cos(6\theta_{ijk}), \quad (5)$$

where θ_{ijk} is the angle in the x - z plane between \mathbf{r}_{ij} and \mathbf{r}_{ik} , the vectors joining the centers of particle i and two of its nearest neighbors, particles j and k . N_i is the number of nearest neighbors to particle i and N_l is the number of particles in the l th layer. A perfect in-plane hexagonal order would give a value of $X_i = 1$. Particles were considered nearest neighbors of particle i if they lay within a distance of $r_{hcp}/0.8$ in the x - z plane and $r_{lay}/3$ in the y direction, where r_{hcp} is the distance between the nearest neighbors in the perfect hexagonal structure and r_{lay} is the distance between 111 layers in the perfect fcc structure.

The average profiles of X are plotted for $T = 0.7, 0.788,$ and 0.85 in Fig. 2 against the displacement y along the surface normal. A homogeneous thermostat has been used for all simulations reported here. The equilibrium melting temperature is 0.907 . The origin along the y axes is defined as the point at which the instantaneous value of X equals 0.5 . Apart from a slight broadening of the interface at the lowest temperature (and highest shear stress), we find very little variation in the interface structure as we move along the nonequilibrium coexistence line.

C. Velocity field and effective boundary conditions

In contrast to the interfacial structure, the profile of the average velocity along the gradient direction exhibits a sig-

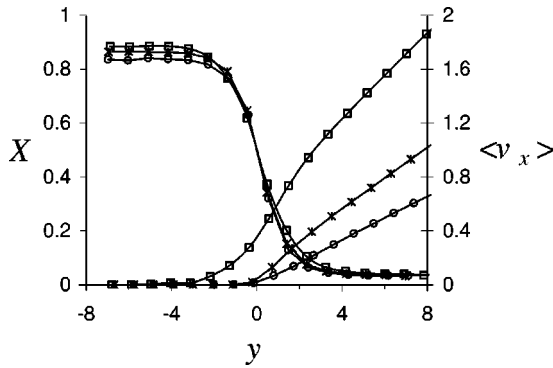


FIG. 2. The profile for the crystalline order parameter X , defined in Eq. (5), and the average velocity $\langle v_x \rangle$ in the direction of the shear flow at $T=0.7$ (squares), 0.788 (crosses), and 0.85 (circles). The profiles have been averaged over 120 000 time steps. The origin in y is defined as the point at which $X=0.5$ in the average structure profile. The velocity $\langle v_x \rangle$ is measured relative to the crystalline wall.

nificant change with temperature and stress. We have calculated the average velocity along the flow direction v_x as a function of y , again measured from an origin fixed on the surface position. In Fig. 2, we also plot the average shear velocity against y at the same three points along the coexistence line. We note two changes as one moves along the nonequilibrium coexistence line towards lower temperatures. First, the velocity field penetrates into regions of higher crystalline order. Second, the gradient of the velocity increases in the liquid adjacent to the surface. This increase in the strain rate occurs within the interfacial region suggesting an enhanced slip associated with the sliding of ordered layers.

We shall quantify surface slip in terms of a “slip length.” To define this length, we extrapolate the velocity field far from the interface to the point where the (extrapolated) velocity equals that of the bulk crystal. This construction is shown in Fig. 3. Typically [6], one would then define a slip length as the distance along the surface normal between this point and the position of the wall. A length of zero corresponds to stick boundary conditions, while a negative length characterizes the degree of boundary slip between crystal and liquid. A creep flow at the wall, indicated schematically in

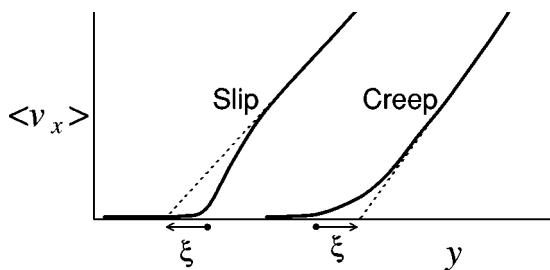


FIG. 3. Qualitative sketches of flow velocity profiles at a diffuse interface for the cases, where (a) slip and (b) creep flow occur in the interface region. The position of the wall boundary as the point where the shear velocity drops below some chosen threshold is indicated. The appearance of negative and positive stick lengths ξ in (a) and (b), respectively, are indicated.

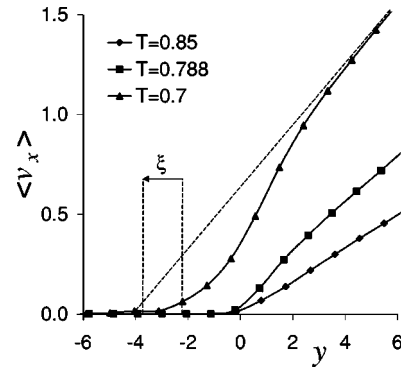


FIG. 4. The graphical estimate of the stick length from the calculated shear profiles at $T=0.7$, 0.788 , and 0.85 .

Fig. 3, would give a positive slip length. In the case of the diffuse interface, there is some ambiguity as to which definition of the interfacial position is the most physically relevant. A definition based on interfacial structure, for example, has no obvious relevance with respect to fluid flow. Instead, we shall define the “hydrodynamic” surface to lie at the point at which the actual velocity difference between crystal and liquid drops first below some small threshold, chosen here to be 0.06. As shown in Fig. 4, the calculated slip lengths at $T=0.7$, 0.788 , and 0.85 are, respectively, 2.4, 1.4, and 1.1. These lengths are considerably smaller than the interfacial profile width of roughly 4, measured from X equal to 90% of the bulk crystal value to X equal 10% of the crystal value. Despite the clearly nonlinear character of the flow field at the lowest temperature, these small slip lengths suggest that the crystal-melt interface behaves like a simple stick boundary. We conclude that the enhanced slip in the liquid side of the interface is almost completely compensated by the creep flow deeper into the crystal.

How does the velocity field correlate with the structural field? In Fig. 5, we combine the information in Figs. 3 and 4 and plot the average velocity (measured with respect to the crystal wall) against the crystal order X for the three state points. We find that, as the temperature decreases (and shear stress increases), slipping occurs at layers of increasing order. We shall define the onset of slipping to be where the average velocity exceeds 0.06. The definition is, of course, arbitrary. We can then determine the maximum value of crystal order, called X_{slip} , at which slipping takes place. The

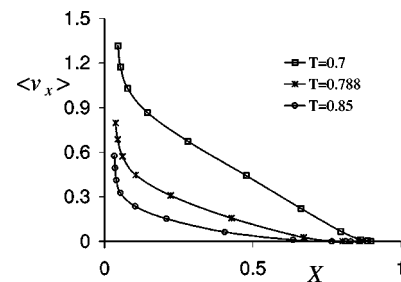


FIG. 5. The average flow velocity $\langle v_x \rangle$ relative to the crystalline wall is plotted against the in-layer order parameter X for $T=0.7$, 0.788 , and 0.85 . The figure highlights the increasing penetration of shear velocity into regions of substantial crystalline order.

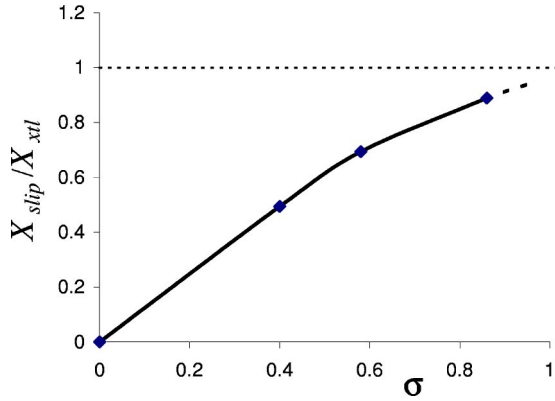


FIG. 6. A plot of X_{slip}/X_{xtl} vs shear stress σ along the coexistence curve.

ratio X_{slip}/X_{xtl} is plotted against T in Fig. 6. We find a steady increase in this ratio with decreasing temperature. As this ratio approaches 1 the penetration depth of the shear flow into the crystal will diverge.

The concept of a penetration depth of the shear flow into the crystal appears to be a useful way of characterizing the nonequilibrium interface. We have defined this length d as the distance between $X(y)=0.1$ and $X(y)=X_{slip}$, as shown in Fig. 6. A plot of the penetration depth d vs the shear stress is shown in Fig. 7. We find that the interface of the Lennard-Jones crystal is penetrated to a depth that increases substantially as the shear stress is increased. We conclude that the nonequilibrium crystal-liquid interface includes a layer of shearing crystal whose thickness increases rapidly with shear stress. Previous simulations of the nonequilibrium phase diagram of a colloidal crystal [7,8] considered the coexistence between a *shearing* crystal and the disordered phase. Light scattering experiments [9] and simulations [7,8] demonstrate that the shearing colloidal crystals become unstable at some critical shear rate. Such an instability would curtail the diverging thickness of the shearing layer at the crystal-liquid interface. Simulations at higher shear stresses will be necessary to understand the role that such an instability might play in the Lennard-Jones system.

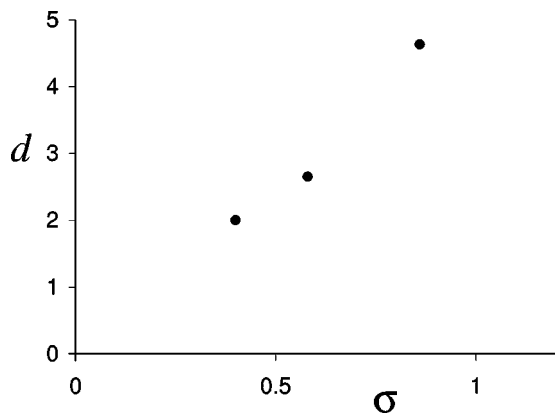


FIG. 7. The penetration depth d (as defined in the text) plotted against shear stress σ .

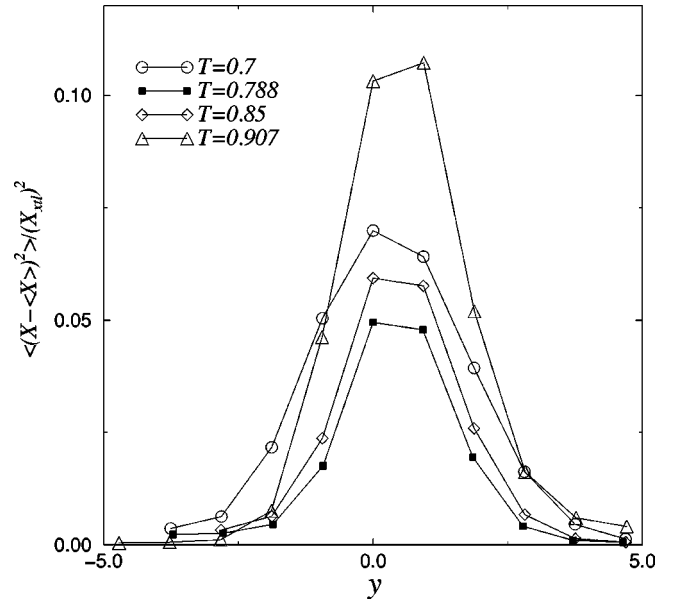


FIG. 8. The variance $\langle (X_i - \langle X_i \rangle)^2 \rangle / (X_{xtl})^2$ of the interfacial structure through the interface at equilibrium ($T=0.907$) and three nonequilibrium states: $T=0.85$, 0.788 , and 0.7 . Note the nonmonotonic temperature dependence of the interfacial structural fluctuations with temperature. The origin of y is chosen here as the position where the average order parameter equals 0.5, i.e., the *average* interfacial position rather than the *instantaneous* position.

IV. FLUCTUATIONS AT THE NONEQUILIBRIUM INTERFACE

In Fig. 8, we plot the variance of the in-layer structure X as a function of the position through the interface, relative to the value of X_{xtl} , the structure in the bulk crystal. Note that a different definition of the zero along the y axes has been used here. The one used in the preceding section would constrain the fluctuation in order at $y=0$ to be zero. In Figs. 8 and 10 we have defined the origin to be the point at which the time average of X equals 0.5. We find a nonmonotonic dependence on the amplitude of structural fluctuations as a function of how far one has moved along the nonequilibrium coexistence line from the point of zero shear stress. Beginning at $T_M=0.907$, the equilibrium coexistence point, the amplitude of the fluctuations at the center of the interface drops sharply as the shear rate of the liquid increases and the temperature decreases. This trend is eventually reversed. At $T=0.7$, the lowest temperature and highest shear stress studied here, the structural fluctuations have increased in amplitude compared with the fluctuations at $T=0.788$. These observations suggest the following picture. The thermal interfacial fluctuations present at equilibrium are suppressed by the combination of liquid shear flow and decreasing temperature. With increasing shear rate and the associated increase in flow penetration into the crystal region, the amplitude of interfacial fluctuations eventually increase as shear-driven fluctuations begin to dominate.

The structural fluctuations of the interface at high liquid shear rates must be strongly coupled to the fluctuations in the shear velocity field in the liquid. There is, of course, no analog to this coupling at the equilibrium coexistence. In Fig.

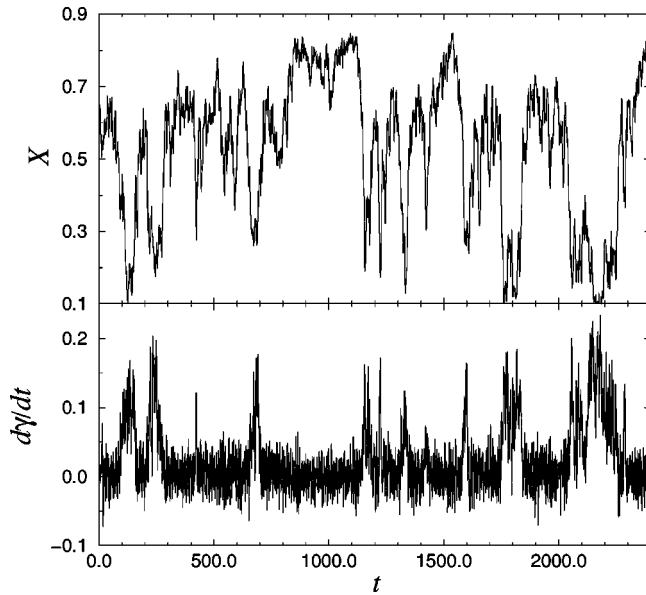


FIG. 9. The time dependence of the structure X and the strain rate $d\gamma/dt$ averaged over a single layer at $T=0.85$ under a homogeneous thermostat. The layer was chosen as the one immediately adjacent (on the liquid side) to the point at which $X=0.5$. Note the clear transitions between stick and slip and the accompanying large structural fluctuations. The strain rate of a single layer was calculated as the difference between the average shear velocity of a layer along the flow direction and its neighbor on the crystal side, divided by the spacing between layers. The data for X and $d\gamma/dt$ have been coarse-grained in time to reduce noise, the average taken over a time interval of 3τ .

9 we have plotted the time dependence of the in-layer structure X and the strain rate $d\gamma/dt$ for a single layer in the nonequilibrium crystal-liquid interface at $T=0.85$ (homogeneously thermostated). This particular layer has a time averaged structural order parameter of slightly less than 0.5 and so represents the behavior at the interface center. The strain rate $d\gamma/dt$ of a layer is calculated as the difference between the average shear velocity of a layer and its neighbor on the crystal side, divided by the spacing between layers. The crystalline order in the selected layer undergoes large and abrupt fluctuations in time. The fluctuations in the strain rate show similar abrupt variations, but of a more bimodal character with the layer either at rest with respect to its more ordered neighbor or slipping at a relatively well-defined rate. This transient stick-slip behavior is strongly correlated with the structural fluctuations. Layer slipping is always accompanied by layer disordering. This correlation can be quantified as a negative cross correlation between fluctuations in order and shear velocity, shown in Fig. 10. Simulations of stick-slip behavior of thin liquid film confined between crystalline walls [10] exhibit a similar correlation between shearing and disorder.

V. EROSION AND THE KINETIC CHARACTER OF NONEQUILIBRIUM COEXISTENCE

The stability of coexistence between any two phases can, in principle, be described in terms of an equality between the

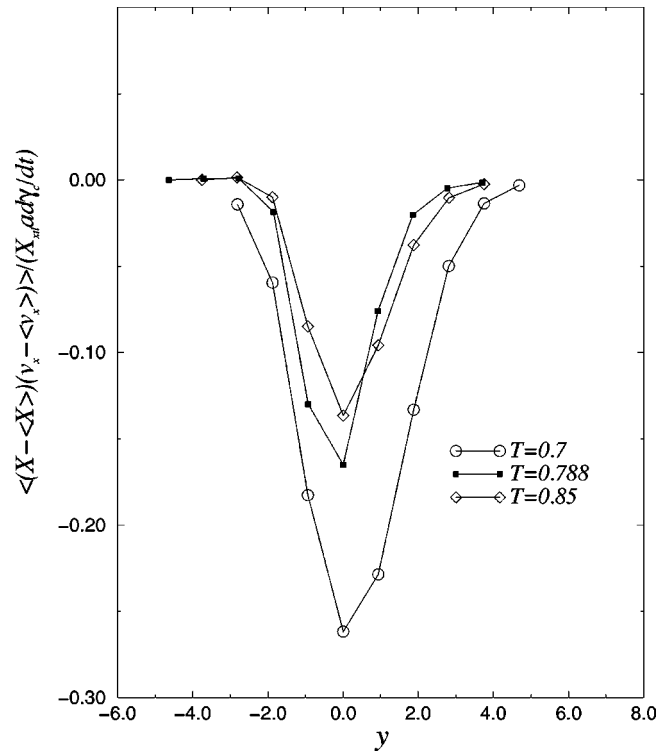


FIG. 10. The cross correlation $\langle (X_i - \langle X_i \rangle)(v_{xi} - \langle v_{xi} \rangle) \rangle / (X_{xil} d\gamma_c/dt)$ between the fluctuations in the structure and the shear velocity through the nonequilibrium interface at $T=0.85$, 0.788, and 0.7. The actual strain rate at coexistence $d\gamma_c/dt$ depends on temperature. Note the increasing negative correlations in the interface associated with the disordering accompanying layer slip.

rates of exchange of material between the two phases across the interface. The thermodynamic prescription of defining coexistence as the equality of the respective chemical potentials is considerably more convenient, since it avoids having to deal with questions of specific kinetic processes, the exact character of the interface, and so on. In the present case involving a crystal and a shearing liquid, however, we have shown [2,3] that no reasonable definition of an “effective” chemical potential for the shearing liquid can account for the observed coexistence with the strained crystal. From the point of view of the kinetic picture of coexistence, this result implies that the rates at which particles fluctuate between the crystal and the shearing liquid depend explicitly on properties of the nonequilibrium interface, in contrast to the situation at equilibrium. In this section, we shall consider a simple treatment of the kinetics of the nonequilibrium crystal-liquid interface to account for the observed coexistence.

The following model involves two major simplifications. The first is to decompose the interfacial kinetics into two separate processes: crystallization governed only by the supercooling, and the mechanical disruption of the interfacial structure governed by the shear flow in the interfacial region. The second assumption, dealt with below, concerns the treatment of the rate of mechanical disruption.

From the first assumption, we estimate the crystallization

rate as simply that expected for a *nonshearing* liquid whose supercooling ΔT is the difference between the equilibrium freezing temperature and the temperature of the supercooled liquid. In Refs. [2,3], we have shown that an increase in the solid chemical potential due to shear strain is insignificant. While this provides some justification for the neglect of the shear stress at this point, the real simplification introduced here is the to neglect the role of the liquid shear flow in calculating this crystallization rate. The idea is that one can “bundle” all of the shear-structure interaction into a separate rate of mechanical disruption of the surface. This conceptual separation of the two interfacial processes draws some modest encouragement (if not actual support) from the intermittent character of flow at the interface, as demonstrated in Fig. 9. After all, the interface exhibits its own *temporal* separation between a state of zero shear flow with small amplitude structural fluctuations and one of significant shear flow with disruption of order.

The mechanical character of the shear-induced disordering at the interface emphasises the essential nonthermal character of the fluctuations involved. The flow field couples quite specifically to certain shear modes of the solid, driving them through to instability. A process in which a liquid disrupts the solid surface against which it flows seems to quite naturally fit the description of *erosion*. The process described here differs from the more familiar examples of erosion in that the liquid here is the melt of the solid. Instead of water over stone, one should think of lava over stone. The greater the proximity to the solid melting point, the smaller the amount of mechanical work the flowing liquid must supply to disrupt the solid. So while conventional erosion is often accompanied by turbulent liquid flow, here the flow is explicitly laminar. (A qualification is needed here. The actual shear rates imposed here, while small in terms of NEMD simulations, still correspond to enormous shear rates of the order of 10^{12} s^{-1} . The stability of the lamellar flow is due to the small dimension of the simulation cell.)

We are unaware of a molecular-level description of erosion. Ajdari [11] has presented a phenomenological model of the shear disruption of aggregates at a wall (or “peeling of the aggregate,” as it is described) by the inclusion of a term in the equation of motion of the interface position that increases linearly with shear stress above some threshold value. Here, we shall estimate the rate of erosion as follows. Forcing the material at the interface to slide is assumed to disrupt ordering, at least with respect to the adjacent solid if not the in-layer order, and so reduce the stability of this material. Such disrupted material will be deemed “eroded.” We neglect here the possible stability of a sliding crystal phase, an issue that certainly deserves to be considered more carefully. We shall assume that the local rate at which the crystalline order is disrupted by shear flow is proportional to the product of the local degree of crystalline order and the local strain rate, that is, $X \dot{\gamma}_{local}$. Erosion, therefore, explicitly involves the penetration of the shear flow into the crystal, as described in Sec. IV. We propose that the overall rate of erosion of the interface is simply the average rate of crystal disruption through the interface, i.e.,

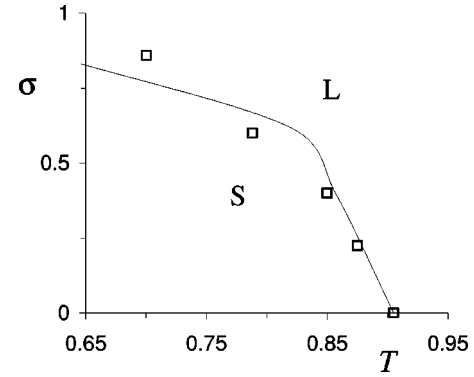


FIG. 11. The temperature dependence of the shear stress (solid line) at coexistence as a function of temperature calculated from the erosion model described in the text. The nonequilibrium coexistence states from simulation are indicated as open squares.

$$\mathcal{R}_{erosion} = C(T) \int_{-\infty}^{\infty} dy X(y) \dot{\gamma}_{local}(y). \quad (6)$$

This expression is presented as the simplest mathematical representation of the fact that erosion occurs only in that volume in which the crystalline order and an appreciable shear rate coexist. The expression makes no claims to embodying any more physics (such as an explicit mechanism of mechanical disruption) than this basic proposal.

Our picture of the nonequilibrium crystal-liquid coexistence is that the state is determined by the balancing of the growth rate driven by the persistent chemical potential difference and the rate at which the shearing melt is eroding the surface. At small undercoolings, the crystallization rate expected for a rough interface is proportional to chemical potential difference between the two phases. Expanding to the lowest order in supercooling $\Delta T = T_M - T$ (and neglecting the contribution from the crystal strain [2]), we can express the crystallization rate \mathcal{R}_{xtl} as

$$\mathcal{R}_{xtl} = B(T) \Delta T. \quad (7)$$

Equating the erosion and crystallization rates results in the following relation between temperature T and shear rate profile $\dot{\gamma}_{local}(y)$ at coexistence:

$$T = T_M - A \int_{-\infty}^{\infty} dy X(y) \dot{\gamma}_{local}(y), \quad (8)$$

where $A = C/B$. A quantitative treatment of crystal growth from the Lennard-Jones melt has been reported by Huitema *et al.* [12], which provides the explicit value of $B(T)$. However, in the absence of any estimate of the rate constant C for erosion, we shall treat the ratio A of kinetic coefficients as a constant to be adjusted to optimize the fit with the observed coexistence curve with the result that $A = 0.45$. We compare the coexistence curve calculated using Eq. (8) with the simulated coexistence points in Fig. 11 and find a reasonable fit. Note that the relation between temperature and the coexistence shear stress in Eq. (8) is implicit through the strain rate

profile. This implicit relation incorporates the details of the flow penetration into the solid.

VI. CONCLUSION

We have examined the crystal-liquid interface along the nonequilibrium coexistence line characterizing a stationary interface between the strained fcc crystal of Lennard-Jones particles and the shearing melt. The shear flow is found to penetrate to a depth that increases significantly as one moves away from the equilibrium coexistence. While shear flow and crystal structure share the same volume, they do not do so at the same time, but rather alternate intermittently between ordered arrest and disordered flow. The shear flow in the interface region can, thus, be characterized by marked stick-slip behavior with the slip accompanied by an abrupt disordering, reminiscent of that observed in stick-slip flow in confined liquid films [10]. A similar intermittent motion has been inferred in the case of low shear rates in “soft” crystalline phases. In their light scattering study of shearing in colloidal crystals, Ackerson and Clarke [9] concluded that at low shear rates the crystal layers “jumped” from registry to registry with respect to the adjacent layers. Nothing in the preceding analysis precludes the behavior reported here for the Lennard-Jones system from applying to the hard sphere model, often used in the context of sterically stabilized colloids.

The erosion model, presented here, highlights the important role that interfaces can play in establishing coexistence under nonequilibrium conditions. This is in contrast to the case at equilibrium where, in the thermodynamic limit, the interface contribution is negligible. The results of this work can be summarized as follows. The diffuse crystal-melt interface represents a mechanically fragile structure, and coexistence under shear cannot occur unless this interface is stable. The separation of the crystallization and erosion processes is an artificial one, and we are currently developing a more systematic theoretical treatment of the solid-liquid coexistence under shear that treats both features within a single consistent framework.

Stable, reproducible shear banding has been reported in simulations of a glass-forming mixture [13]. While this nonequilibrium coexistence involves a diffuse interface (as determined by the shear velocity profile) similar to the interface described in this paper, there are some important differences between the two phenomena. The shear banding of the model glass occurs in the absence of long range order in either “phase”; it involves nonlinear response of the bulk phase and it lacks the true plateau in the stress-strain rate curve, characteristic of the two-phase coexistence. It would be interesting to see if the shear banding in the glass could be described in terms of some sort of coexistence between phases distinguished by local order.

The nonequilibrium coexistence between crystal and melt should be relatively straightforward to observe experimentally. Such experiments would be particularly interesting in terms of the insight they could provide on the mechanical properties of the interface. Our results suggest, for example, that the application of a shear stress roughly half that of the yield stress will result in a 6% decrease in the coexistence temperature. To avoid nonlinear behavior in the liquid, low stresses and/or high viscosities are optimal. Soft solids with low yield stresses are therefore interesting candidates. The surfactant dodecyltrimethylammonium chloride forms a stiff cubic phase in a 50 wt% aqueous solution [14]. The cubic phase disorders to an isotropic micellar phase above the melting point 90 °C and has a yield stress of the order of 10³ Pa. Scaling our simulation results with these values, we predict that, at shear stresses of around 500 Pa, we would see the cubic-isotropic coexistence temperature lowered by about 20 °C.

ACKNOWLEDGMENTS

One of us (P.H.) gratefully acknowledges many helpful discussions with Greg Warr. This work has been supported by an Institutional Grant from the Australian Research Council and generous grants of computer time from the Australian National University Supercomputer Facility.

-
- [1] P. Thompson and M. Robbins, *Phys. Rev. A* **41**, 6830 (1990); P. Thompson and S. Troian, *Nature (London)* **389**, 360 (1997); A. Jabbarzadeh, J.D. Atkinson, and R.I. Tanner, *J. Chem. Phys.* **110**, 2612 (1999); M. Ciepak, J. Koplik, and J. Banavar, *Phys. Rev. Lett.* **86**, 803 (2001).
 - [2] S. Butler and P. Harrowell, *Nature (London)* **415**, 1008 (2002).
 - [3] S. Butler and P. Harrowell, *J. Chem. Phys.* **118**, 4115 (2003).
 - [4] P.D. Olmsted and C.Y.D. Lu, *Phys. Rev. E* **60**, 4397 (1999).
 - [5] D. Evans and G. Morriss, *Statistical Mechanics of Nonequilibrium Liquids* (Academic, Sydney, 1990).
 - [6] R.I. Tanner, *Engineering Rheology* (Oxford University Press, London, 2000).
 - [7] M. Stevens and M. Robbins, *Phys. Rev. E* **48**, 3778 (1993).
 - [8] S. Butler and P. Harrowell, *J. Chem. Phys.* **103**, 4653 (1995).
 - [9] B.J. Ackerson and N.A. Clarke, *Phys. Rev. A* **30**, 906 (1984).
 - [10] P.A. Thompson and M.O. Robbins, *Science (Washington, DC, U.S.)* **250**, 792 (1990).
 - [11] A. Adjari, *Phys. Rev. E* **58**, 6294 (1998).
 - [12] H. Huitema, M.J. Vlot, and J.P. van der Eerden, *J. Chem. Phys.* **111**, 4714 (1999).
 - [13] F. Varnik, L. Bocuquet, J.-L. Barrat, and L. Berthier, e-print cond-mat/0208485.
 - [14] R. Balmbra, J.S. Clunie, and J.F. Goodman, *Nature (London)* **222**, 1159 (1969).